International Journal of Science and Research (IJSR)
ISSN (Online): 2319-7064
Impact Factor (2012): 3.358

Performance Analysis of Stain Less Steel Conical Probe Using Levenberg-Marquette Algorithm

J.V Murugalal Jeyan[1], Akhila Rupesh[2]

Department of Aeronautical Engineering, Rajadhani Institute of Engineering and Technology,
Nagaroor,Attingal, Thiruvananthapuram 695102, India

Abstract: ***The multi hole conical probe is extensively employed in the fluid fields for estimating the overall and static pressure and velocity of the vibrant fields. The probe is formed by stainless steel which is utilized in the wind tunnel to determine the static and total pressure of the fluid fields. The probe is engaged to assess their efficiency in execution in the concurrent surroundings at diverse Mach number situations and the yields are calculated according to displacement and stress. The innovative artificial neural network is effectively employed to forecast the accomplishment of the probe by making use of the Levenberg-Marquette algorithm of the artificial neural network, which is applied in the artificial neural network to estimate the yields of the probe and the outcomes are subjected to analysis and contrast with the Conjugate Gradient with Beale (CGB) algorithm, Variable Learning Rate Gradient Descent (GDX) algorithm and Scaled Conjugate Gradient (SCG) algorithm of the artificial neural network. The MATLAB software is performed to assess the efficiency of the artificial neural network for the probe.***

Keywords: multi-hole probe, materials, artificial neural network, Levenberg-Marquette algorithm

1. Introduction

Multi-hole pressure probes have emerged as highly efficient devices for multidimensional flow field estimations. They furnish sufficient data of flow such as velocity, direction, in addition to overall and static pressures at the point of interrogation. They are endowed with the quality of being reasonably vigorous, making them suitable for employment for flow metrology in ruthless situations. [1] The divergence between the pressures sensed on various faces of a probe is linked to the velocity vector and static pressure. The multi-hole pressure probes have been extensively employed for estimating the time-averaged flow velocity together with the pitch and yaw angles of the flow related to the probe.[2]The static pressure ports have to be positioned reasonably at a distance downstream of the probe tip, to steer clear of estimating incorrect pressures on account of the adverse effect of the shock. The shape of the shock in front of the probes manages the closest distance they can be positioned at, and thrusts a basic limit on the spatial resolution of the dimensions.[3] Stochastic computational fluid dynamics (CFD) techniques are essential for successfully tackling fluid dynamics dilemmas that entail reservations linked with the modeling of the bona fide life situations like the working environments, the geometry, primary or boundary situations furnished into the solver as input.[4] With an enhancement in number of holes, the range of the angle of incidence that can further be calculated with the probe goes up. Moreover, there are probes which have one pressure port, which is continuously twisted inside the probe. The number of holes which are employed for three dimensional flow dimensions must be at least a minimum of four. [5] The transonic wind tunnel at the Department of Aerodynamics is a comparatively tiny installation intended to conduct tests at a transonic pace. The Mach number of the main flow is capable of being realized in the course of the tests. [6] The application of multi-hole probes necessitates a cautious calibration with the achievement of three-dimensional data. The pressure probe can be performed in two distinct ways such as the nulling or the non-nulling method.[7] The calibration surfaces related to the four calibration coefficients together with identified pitch and yaw are employed to build up a parametric link between the pressures at the five pressure taps of the probe and the magnitude and direction of the velocity of air.[8] The measuring tool employed for calculating velocities at various locations is the unique multi hole probe with the conical diameter. The sensing head is conical shaped to let the probe shaft without in any way upsetting the probe tip direction.[9] The calibration of multi-hole pressure probes is gathered from the concept of optimal design of experiments (DoE) and the captioned technique is extended to the calibration of multi-sensor hot-wire probes.[10] Alberto Calia*et al.* [11] have astoundingly advocated an amazing approach for Multi-hole probe and amplification algorithm which is employed for calibrating the air data emerging from the CFD by making use of the neural systems and refurbished the data. The resultant outcomes illustrate the fact that the fault value has decreased the air speed for 30m/s. LI Yuhong*et al.* [12]have logically put forward the probe dimensions for Reynolds number finding, with the Mach number enhancements. The outcomes indicate that the expression α=20 gives the precise outcome for the Mach number in subsonic flow. John. F. Quindlen*et al.* [13] formulated the fantastic technique for Flush Air Data Sensing for Soaring-Capable UAVs by means of the artificial neural network. The outcomes illustrate the fact that the fault value of the air speed is below 0.2 m/s with α=.6^{o}. E.Denti*et al.* [14] have excellently promulgated an air data calculation by means of fault tolerant algorithms. The outcomes clearly exhibit the fact that the air data system cuts down the error value to 6 m/s. HUI-YUAN FAN et al. [15] have proficiently put forward an innovative technique viz. CFD-based diffuser optimization method which is employed for calibrating the pressure co-efficient. The outcomes demonstrate the fact without any iota of doubt that when the SVM technique is contrasted with the artificial neural network based technique, the ANN technique performs far better than SVM technique

for calibrating the pressure co-efficient, achieving a value of 0.0286.

2. Proposed Methodology

The proposed artificial neural network is trained by the input parameters in various conditions and the trained network is tested by the same type of input parameters for future usage. It is used to find out the output of the probe for different materials at different input conditions. The input parameters such as material properties, Mach number and pressure are given to the trained artificial neural network and the outputs obtained in terms of displacement and stress by using the testing data sets. The Levenberg-Marquardt algorithm is used in the artificial neural network process to train the network for the given input conditions and find out the output approximately equal to the calculated value.

2.1 Artificial Neural Network

The Artificial neural networks are the programmed computational models which are usually presented as systems of interconnected neurons that can compute values from inputs by feeding data through the network. Artificial neural networks are flexible and adaptive, learning and adjusting with each different internal or external stimulus.

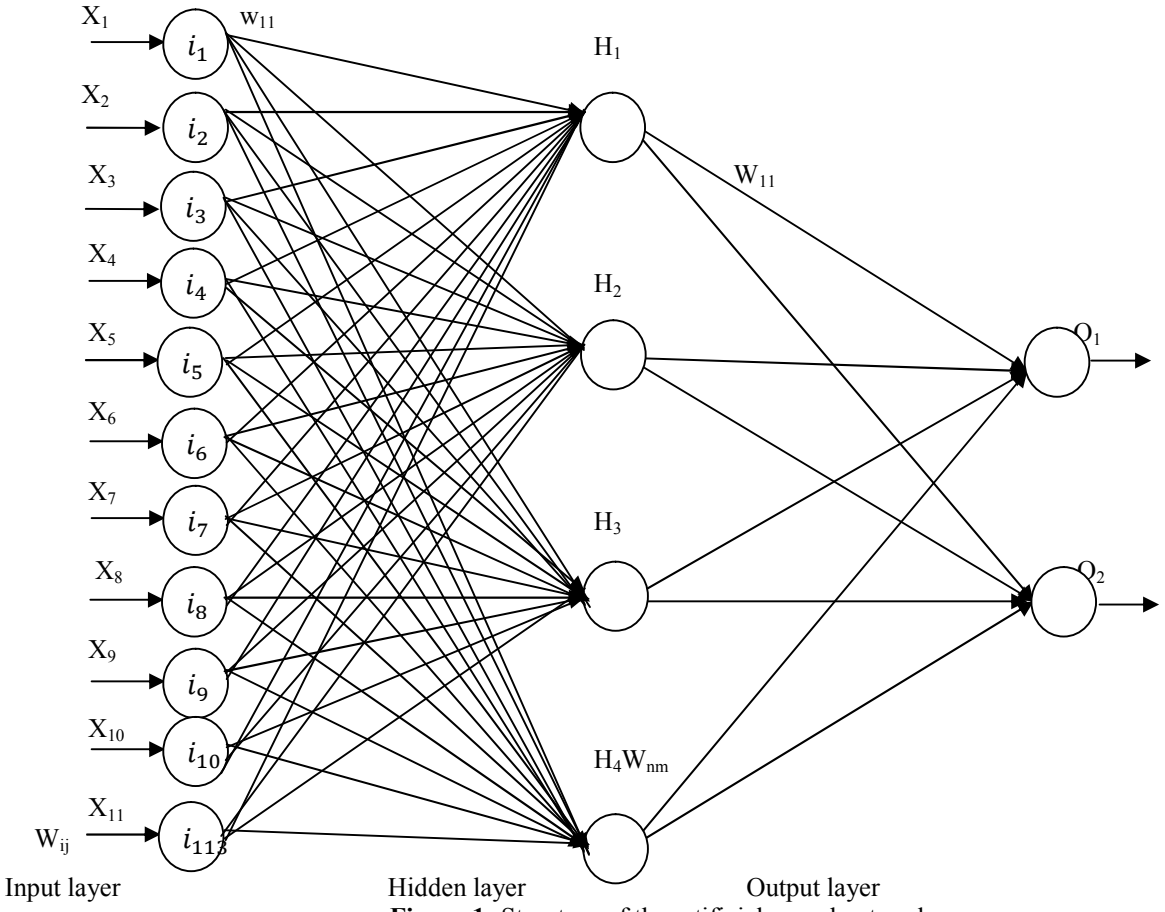

Figure 1: Structure of the artificial neural network

The basic architecture of feed-forward back-propagation based artificial neural network is shown in Figure 1. It has the multi-layer artificial neural network which consists of 3 layers such as input layer, hidden layer, and output layer. Each layer contains a number of the neurons and all layers are connected by the neurons. Based on the connections, the ANN networks are of two type's viz. feed forward network and feedback network. Here, the feed forward network is used. In this network, the signal or data is transmitted from front to back with balanced flow and there are no reverse transmissions of the data flow. The three layers are explained below:

2.2 Input layer

The input layer contains a number of neurons. All input layer neurons are connected with the hidden layer neurons. It has twelve inputs and the input neurons are named as $i_1,i_2 \ldots i_{12}$. The inputs are $X_1,X_2 \ldots X_{12}$ and each neuron possesses the weight which is represented as the i^{th} input layer neuron connected with the j^{th} neuron of the hidden layer like $W_{11},W_{12},W_{13},W_{14},W_{21},W_{22} \ldots W_{ij}$.The basic function is calculated by using the following formula:

$$H_z = \sum_{i=1}^{n} X_i W_{ij} \quad \text{---------- (1)}$$

z=1, 2, 3, 4. i=1, 2, 3, 4…12. j=1,2,3,4.

Where, H=Basic function of hidden neurons, z=number of hidden units, w= weight of the input layer neurons, X=input values which are X_1 =Young's Modulus (E), X_2= Poisson's Ratio (NU), X_3=Yield Strength,X_4=Ultimate Tensile Strength, X_5=Initial Strain,X_6=Hardening Exponent,X_7=Strength Coefficient, X_8= Thermal

Conductivity (K),X_9=Specific Heat (CP), X_{10}=Mach number and X_{11}=Pressure. i= Number of input neurons, j= number of hidden neurons.

2.3 Hidden layer

The hidden layer contains a number of neurons which are named as $h_1,h_2….h_n$. The hidden layers are connected with the output layer by using the neurons. The activation function is calculated by the following equation:

$$\sigma(H_z)=\sum_{i=1}^{z}1/(1+\exp(-H_z)) \quad \text{---------- (2)}$$

z=1, 2, 3, 4
Where, Hz is output of the basic function

2.4 Output layer

The output layer has a number of neurons. They are named as $o_1,o_2,….o_n$. It has two outputs which are the displacement and stress. The hidden layer neurons are connected with the output layer by the neurons. Each link has a weighted value such as $W_{11,}$ W_{12}, $W_{13}…w_{nm}$.

The basis function of the Output units is expressed by the Equation:

$$O_k=\sum_{i=1}^{n} W_{nm}\sigma(H_z) \quad \text{---------- (3)}$$

k=1, 2. n=1,2,3,4. m=1,2.

The Activation function of the Output units is given by the Equation:

$$\sigma(\delta_n)=\sum_{i=1}^{n}1/(1+\exp(-O_k)) \quad \text{---------- (4)}$$

n=1,2

The Levenberg-Marquardt algorithm is used to find out the minimized error value of the trained function values. It has the following steps:

First, the error term for the hidden and output units is found out by the following equation:

$$E(O_n)=\frac{1}{H_d}\sum_{i=1}^{H_d} D_n-Z_n \quad \text{---------- (5)}$$

Where, n=number of outputs, H_d=Number of neuron in hidden unit, Dn=Desired output, Zn=Obtained output (Activation function output for output unit)

The error term for the hidden unit by using the following formula:

$$\delta_{H_k}=h_k(E)*(1-h_k(E))*O_k \quad \text{---------- (6)}$$

k=1,2,3,4

$$h_k(E)=\sum_{i=1}^{n} W_i*E(O_n) \quad \text{---------- (7)}$$

Where, k=1, 2, 3, 4
Where, Wi=Weight of the output unit and E (O_z) =Error term of the output unit.
The following equation is used to calculate the new weight adjustment value for minimized error value.

$$\Delta_n^h=\eta\delta_{H_n}x_i \quad \text{---------- (8)}$$

$$\Delta_n^o=\eta*E(O_n)*\sigma(H_z) \quad \text{---------- (9)}$$

Where, η is the learning factor (0.2 to 0.5), δ_{H_n} = error term for the hidden unit, x_i= input value($X_1,X_2,…X_{12}$), $\sigma(H_z)$ =activation function of the hidden unit.
The new weight is calculated by using the formula

$$W_i^{h,new}=W_i+\Delta_n^h \quad \text{---------- (10)}$$

$$W_i^{o,new}=W_i+\Delta_n^o \quad \text{---------- (11)}$$

The new weight is used to find out the minimum error output value of the train values.

When the minimum error values are obtained, then the testing values are tested with the minimized error values for getting the actual output values. The following pseudo code shows the artificial neural network process:

Start

Assign input value for each parameter as X_1, X_2…….
X_{11}
Assign weight for each input parameter.

Calculate the basis function and activation function for hidden layers such as H_1, H_2, H_3, H_4 and $\sigma(H_1)$, $\sigma(H_2)$, $\sigma(H_3)$, $\sigma(H_4)$ respectively.

$$H_n = X_n w_n$$

$$\sigma(H_n) = 1/(1+\exp(-H_n))$$

Evaluate the basis function and activation function for outputs such as O_1, O_2 and $\sigma(\delta_1)$, $\sigma(\delta_2)$, respectively.

$$O_n = w_{n+1}H_1 + w_{n+2}H_2 + ... + w_n H_n$$

$$\sigma(\delta_n) = 1/(1+\exp(-O_n))$$

Find the error term for hidden unit and output unit by using Levenberg-Marquardt back propagation algorithm.
Calculate the change in weight

$$\Delta_n^o = \eta * E(O_n) * \sigma(H_n)$$

Evaluate the new weight as

{
If

Δ_n^o is the tolerable error value

then

stop process

else

compute solution with new weight

}
Stop

3. Results and Discussions

The innovative artificial neural network method is executed in MATLAB for stainless steell permutations of the probe. The input constraints are furnished to the artificial neural network and the yields obtained by means of using various algorithms of the artificial neural network. Figure 1 vividly illustrates the artificial neural network employing MATLAB in the course of operation.

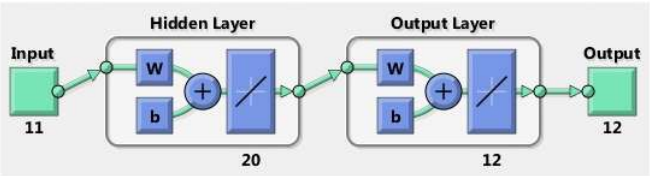

Figure 1: Artificial neural network using MATLAB

3.1 Performance analysis

The ensuing data effectively reveals the execution estimation graph for Stainless steel. The input is guided for the output and experimented by the testing data sets. Four different kinds of algorithms are employed for guiding the artificial neural network by the input constraints and their production accomplishments are analyzed by the graphs

3.2 Stainless steel

Table 1 depicts the performance analysis graph for the stainless steel material employing diverse algorithms. The input constraints are furnished to the artificial neural network and the resultant yields are assessed by means of the MATLAB program.

Table 1: Performance analysis for Stainless steel

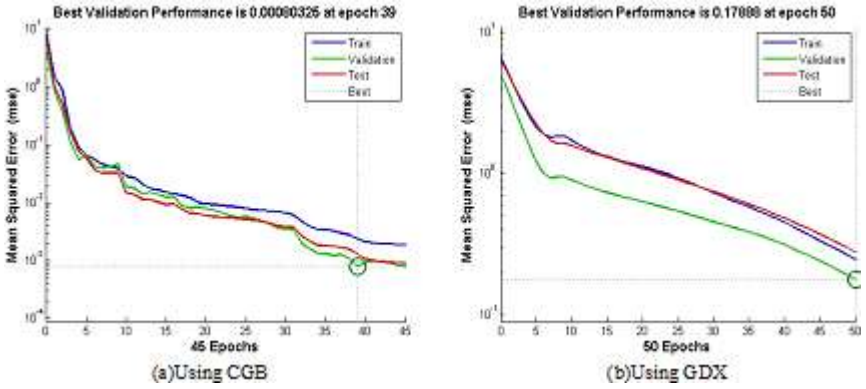

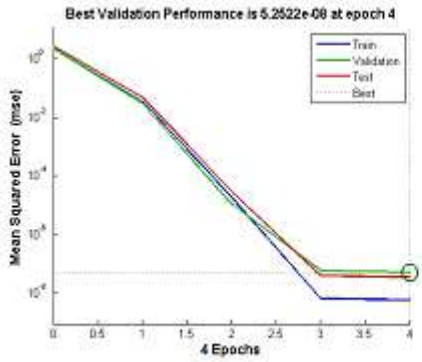

(c)Using LM

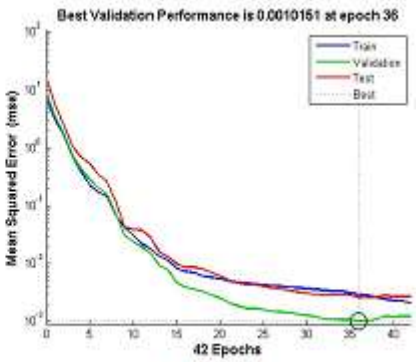

(d)Using SCG

Figures (a), (b), (c) and (d) effectively exhibit the excellent execution of the Stainless steel material with the assistance of the Conjugate Gradient together with Beale (CGB) algorithm, Variable Learning Rate Gradient Descent (GDX) algorithm, Levenberg-Marquardt (LM) algorithm and Scaled Conjugate Gradient (SCG) algorithm. With the help of these figures, the artificial neural network is guided, experimented and authenticated by the input constraints and the ensuing yields are plotted. It is crystal clear from these figures that the yields are converged at iteration 39 with minimum error value 0.00080325 for CGB, iteration 50 with minimum error value0.17888 for GDX, iteration 4 with minimum error value 5.2522e-08 for LM and iteration 36 with minimum error value0.0010151 for SCG. These yields corroborate the fact that the Levenberg-Marquardt algorithm ushers in the minimum error with the minimum iterations.

Regressive Analysis:

3.3 Stainless steel

The ensuing figure illustrates the regressive analysis for stainless steel. With the aid of these figures, all processes such as training, testing, validation are estimated independently for the point which is more or less equal to zero with minimum tolerable error value.

Table 2: Regressive analysis for Stainless steel

Algorithm	Training	Testing	Validation	All
CGB (a)	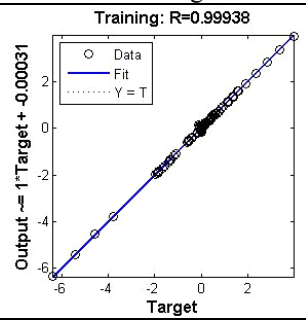	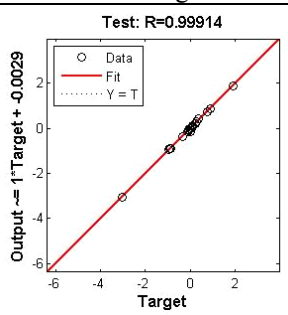	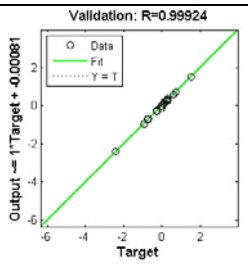	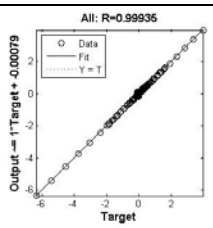
GDX (b)	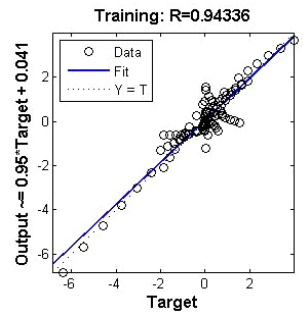	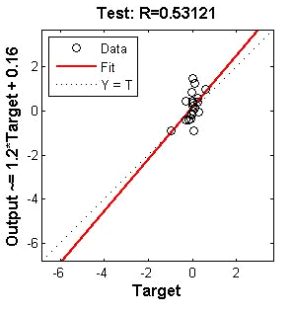	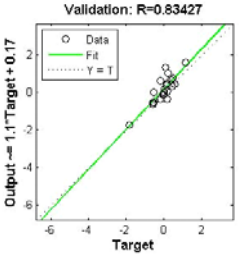	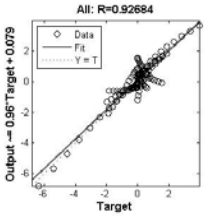
LM (c)	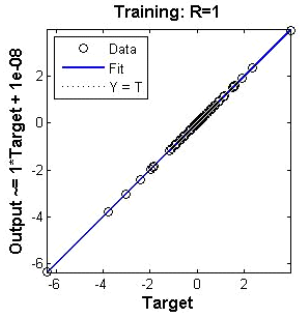	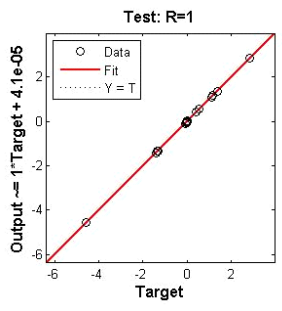	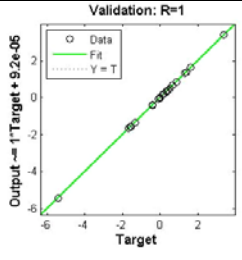	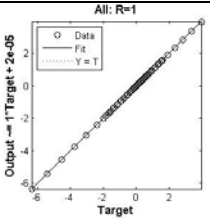

SGC (d)	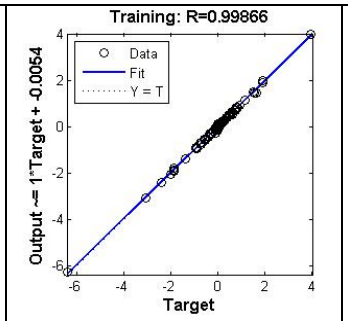	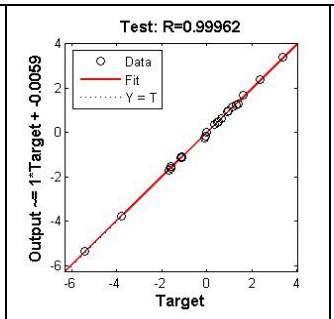	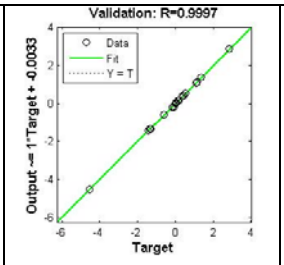	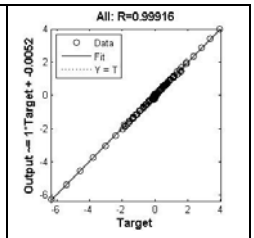

Figures (a), (b), (c) and (d) illustrate the regressive analysis of the Stainless steel material. The figures are plotted between the target value and the output value with the tolerance. Each graph depicts the various algorithms employed for the training value, testing value, validation value and integrated all the three data sets. Figure (i) demonstrates the Conjugate Gradient with Powell/Beale algorithm employed for the aluminum material which indicates the training value as almost equal to zero when R=0.99938 with a tolerance value of +0.00031. The aluminum material indicates the testing value as more or less equal to zero, in the case of R=0.99914 with a tolerance value of +0.0029. The validation value for the future reference is around zero when R=0.99924 with a tolerance value of +0.00081. All the three training, testing and validation are combined which is more or less equal to zero, when R=0.99935 with a tolerance value of +0.0079. The above explanations are replicated for the residual three algorithms for which values are furnished against each algorithm. The Variable Learning Rate Gradient Descent (GDX) algorithm represented by Figure (j) is employed for the Training process R=0.94336 with tolerance +0.041, Testing process R=0.53121 with tolerance +0.16, Validation process R=0.83427 with tolerance +0.17 and the combined process R=0.92684 with +0.079. The Levenberg-Marquardt algorithm shown by Figure (k) is employed for the Training process R=1 with tolerance +1e-08, Testing process R=1 with tolerance +4.1c-08, Validation process R=1 with tolerance +9.2e-05 and the integrated process R=1 with +2e-05. The Scaled Conjugate Gradient algorithm depicted by Figure (l) is employed for the Training process R=0.99866 with tolerance +0.0054, Testing process R=0.99962 with tolerance +0.0059, Validation process R=0.9997 with tolerance +0.0033 and the amalgamated process R=0.99916 with +0.0052.

4. Conclusion

The stainless steel probe is used to analyze its performance in the real time experiments and their outputs in terms of displacement and stress are analyzed. From this material performance analysis, the stainless steel material is found to yield the best results.The artificial neural network technique is implemented on the experimental data sets for the displacement and stress outputs of the probe with different training algorithms such as Levenberg-Marquette (LM) algorithm, Conjugate Gradient with Beale (CGB) algorithm, Variable Learning Rate Gradient Descent (GDX) algorithm and Scaled Conjugate Gradient (SCG) algorithm. The outputs are computed by using the four different training algorithms and the results are compared with the data sets and the output results are found to be approximately equal to the data set values. From this, it is clear that the Levenberg-Marquette algorithm has been able to furnish the best result with minimum error value compared with those of the other algorithms. In future, the researchers will be using this paper as platform for analyzing the material performance with their own techniques and will utilize it for their research works.

References

[1] V.Malviya, R.Mishra, and E.Palmer, "CFD Investigation on 3-Dimensional Interference of a Five-Hole Probeinan Automotive Wheel Arch" Journal of Advances in Mechanical Engineering, Vol.10, 2010.

[2] Simon Watkins, PeterMousley, and GioacchinoVino, "The Development and Use of Dynamic Pressure Probes with Extended Cones of Acceptance (ECA)" in proceedings of 15th Australasian Fluid Mechanics, pp.13-17, Sydney, 2004.

[3] L. Maddalena,S.Hosdery,A.M.Bonanos,andP.E.Dimotakis, "Extended Conical Flow Theory for Design of Pressure Probes in Supersonic Flows with Moderate Flow Angularity and Swirl" in proceedings of AIAA Aerospace Sciences, Florida, January 2009.

[4] SerhatHosder and Luca Maddalena, "Non-Intrusive Polynomial Chaos for the Stochastic CFD Study of a Supersonic Pressure Probe", in proceedings of 47th AIAA Aerospace Sciences, Florida, January 2009.

[5] N.Wildmann,S. Ravi, and J.Bange, "Towards higher accuracy and better frequency response with standard multi-hole probes in turbulence measurement with Remotely Piloted Aircraft (RPA)" Atmospheric Measurement Techniques, Vol.6, pp.9783-9818,2013.

[6] Witold.c.selerowicz,"Prediction of transonic wind tunnel test section geometry – a numerical study" Journal of the archive of mechanical engineering,Vol.57,No.2,2009.

[7] Ricardo Wallace M. Ferreira, Danielle R. S. Guerra, and Daniel Onofrede Almeida Cruz, "PRESSURE PROFILE OFA CURVED CHANNELBY A MULTIHOLE PRESSURE PROBE" in proceeding of COEBM, 19th International Congress of Mechanical Engineering, Brasília,November 5-9, 2007.

[8] V Malviya, R.Mishra, E.Palmer, and B.Majumdar, "CFD Based Analysis Of The Effect Of Multi-Hole Pressure Probe Geometry On Flow Field Interference" pp. 113-122, 2007.

[9] E.Karunakaran, Ganesan.V,"Mean flow field measurements in an axis-symmetric conical diffuser with and without inlet flow distortion" Journal of Engineering and materials science, Vol.16, pp.211-219, 2009.
[10] Stephen C. McParlin, Samantha. S. Ward, and David M. Birch, "Optimal calibration of directional velocity probes", in proceedings of AIAA Aerospace Sciences, Texas, January, 2013.
[11] Alberto Calia, Roberto Galatolo, Veronica Poggi, and Francesco Schettini, "Multi-hole probe and elaboration algorithms for the reconstruction of the air data parameters" Journal of IEEE Indusial Electronics, pp.944-948, July 2008.
[12] LI Yuhong and Bohn D, "Numerical Investigation of the Influence of Reynolds Number on Probe Measurements", Journal of TSINGHUA SCIENCE AND TECHNOLOGY, Vol.5, No.4, pp.400-403, 2000.
[13] John. F. Quindlen and Jack W. Langelaan,"Flush Air Data Sensing for Soaring-Capable UAV", in proceedings of AIAA Aerospace Sciences, Texas,January,2013.
[14] "Fault Detection and Fail-Safe Operation with a Multiple-Redundancy Air-Data System", in proceedings of AIAA, Toronto, January, 2010.
[15] HUI-YUAN FAN, GEORGE S. DULIKRAVICH, and ZHEN-XUE HAN, "Aerodynamic data modeling using support vector machines" Journal of Inverse Problems in Science and Engineering,Vol.13,No.3,pp.261-278,2005.